Article

Sensitivity analysis and parameter estimation for evaluating the impact of water pollution on aquatic species

Christopher David Ngalya[1,2], **Silas Mirau**[1], **Maranya Mayengo**[1]
[1]Nelson Mandela African Institution of Science and Technology, Arusha, Tanzania
[2]College of Business Education, Dodoma, Tanzania
E-mail: christophern@nm-aist.ac.tz

Received 5 April 2025; *Accepted 10 May 2025*; *Published online 21 May 2025*; *Published 1 December 2025*

Abstract
Aquatic ecosystems are highly sensitive to changes in environmental conditions, making it essential to identify the key factors that influence the dynamics of species populations. This study introduced a nonlinear mathematical model, analyzed it, and identified key sensitive parameters that were used in assessing the impact of water pollution on aquatic ecosystems. Global sensitivity analysis was conducted to determine the parameters significantly impacting aquatic species populations. Parameters were estimated using the least squares method, while sensitivity analysis was performed via Partial Rank Correlation Coefficient (PRCC) and Latin Hypercube Sampling (LHS). Parameters related to organic pollutant growth rates, pollutant absorption rates, and oxygen penetration were identified as positively affecting aquatic species populations by enhancing nutrient availability and metabolic activity. Conversely, competition and inorganic pollutant discharge were found to impact aquatic populations negatively. These findings highlight the critical role of managing sensitive parameters such as pollutants and competitive interactions to maintain and improve the health of aquatic ecosystems.

Keywords aquatic species; global sensitivity; dissolved oxygen; mathematical model; pollutants.

Computational Ecology and Software
ISSN 2220-721X
URL: http://www.iaees.org/publications/journals/ces/online-version.asp
RSS: http://www.iaees.org/publications/journals/ces/rss.xml
E-mail: ces@iaees.org
Editor-in-Chief: WenJun Zhang
Publisher: International Academy of Ecology and Environmental Sciences

1 Introduction

Aquatic ecosystems are vital to the health of the planet, providing essential services such as water purification, flood regulation, and habitat for a diverse range of species (Geist and Hawkins, 2016). These ecosystems support a multitude of ecological functions and processes that are critical for maintaining biodiversity and the overall health of the environment (Cadotte et al., 2011). Aquatic ecosystems include rivers, lakes, wetlands, estuaries, and oceans, each hosting unique species and ecological dynamics. However, these ecosystems are increasingly threatened by pollution from industrial, agricultural, and urban sources (Hader et al., 2020).

Pollution in aquatic environments has been a growing concern for decades, with numerous studies highlighting its adverse effects on water quality and aquatic life (Hader et al., 2020; Bashir et al., 2020).

Inorganic pollutants include heavy metals such as mercury, lead, and cadmium, which originate from industrial discharges and mining activities, are known to bioaccumulate in aquatic organisms, causing toxic effects at various trophic levels (Ali et al., 2019). These metals can bind to cellular components, disrupting metabolic processes and leading to cellular damage, reproductive failure, and death in severe cases (Rainbow, 2007; Su et al., 2014). When organic matter enters a water body, it integrates into the food web, enhancing nutrient availability for native microorganisms and potentially benefiting the entire aquatic ecosystem(Okeke et al., 2022). Excessive nutrients from agricultural runoff lead to eutrophication, resulting in hypoxic conditions that threaten fish populations and reduce biodiversity (Zhang and Zhang, 2007; Jan et al., 2022). Nutrients such as nitrogen and phosphorus promote the excessive growth of algae, leading to algal blooms (Wurtsbaugh et al., 2019). When these blooms die and decompose, the decomposition process depletes oxygen in the water, creating hypoxic or anoxic conditions that can cause massive die-offs of fish and other aquatic organisms (Sarma and Kumar, 2024). Eutrophication also disrupts the balance of aquatic ecosystems, favoring the growth of certain species over others and reducing overall biodiversity (Lucas and Deleersnijder, 2020).

Environmental modeling has become an essential tool for understanding and managing the impacts of pollutants on aquatic ecosystems (Lucas and Deleersnijder, 2020). Various modeling approaches, including deterministic, stochastic, and mechanistic models, have been developed to simulate the behavior and fate of pollutants, as well as their effects on aquatic species. Mathematical models have been widely used to assess the effects of pollutants on aquatic ecosystems (Shi et al., 2023). The study by Tiwari et al. (2017) analyzed the impact of organic and inorganic pollutants on fish survival but overlooked the role of aquatic plants in oxygen production. This represents a significant gap, as aquatic plants not only contribute to oxygen enrichment but also serve as a food source for aquatic organisms. Similarly, Misra (2011) investigated dissolved oxygen depletion due to algal blooms, incorporating nutrient-algae interactions based on Holling Type-III dynamics. However, this model primarily addressed nutrient dynamics without considering the combined influence of multiple pollutants. The model developed by Shukla et al. (2008) examined the simultaneous effects of water pollution and eutrophication on dissolved oxygen levels, revealing a greater oxygen reduction when both factors were present. Nevertheless, it did not explore the long-term consequences of toxicants on fish populations. Further research by Kumar et al. (2016) focused on the effects of toxicants on biological populations, underscoring the need for regulating toxic emissions, but it lacked an assessment of the wider ecological and human health implications. Additionally, the study by Chaturvedi et al. (2017) employed a nonlinear differential equation model to examine nutrient-driven species growth, yet it did not account for interactions between pollutants and other ecological components. More importantly, previous studies have failed to assess key sensitive parameters. Sensitivity analysis and parameter estimation are vital tools for refining these models (Computing, 2004; Yang, 2017).

This research addresses these critical gaps by integrating aquatic plants as a crucial component in oxygen dynamics and incorporating sensitivity analysis to evaluate the most influential parameters affecting ecosystem stability. By considering the intricate relationships among pollutants, dissolved oxygen, bacteria, and fish populations, the study provides a more comprehensive perspective on the effects of water pollution and offers a refined approach to identifying the most critical factors driving ecosystem health.

2 Material and Methods

2.1 Modal descriptions

The model explores the dynamics of pollutants in aquatic ecosystems, distinguishing between organic (P_0) and inorganic (P_i) substances. It incorporates other variables like bacteria density (B), aquatic plants density (such as algae and water hyacinth) (A), dissolved oxygen concentration (C)and fish density (F).

Pollutants enter the water body at rates of Q_1 (inorganic) and Q_2 (organic) and degrade at rates μ_1 and μ_2 respectively. Bacteria thrive on organic pollutants, increasing their population, while fish experience reduced growth due to the ingestion of inorganic pollutants. Bacteria undergo natural mortality at a rate $\mu_6$and are subject to intra-species competition characterized by λ_{20}. Similarly, aquatic plants face natural mortality at a rate μ_3 and intra-species competition represented by λ_{30}. Dissolved oxygen (C) is replenished at a rate Λ_1, but also naturally decreases at a rate λ_4. Additionally, oxygen facilitates the decomposition of bacteria into organic matter at the rate β_{02}. Fish growth critically depends on the dissolved oxygen levels. It is negatively affected by both direct ingestion of inorganic pollutants and the indirect reduction of oxygen caused by the presence of organic pollutants. Fish are also subject to natural mortality at a rate μ_5Intra-species competition at the rate λ_{10}, and toxin-induced mortality from inorganic pollutants at a rate θ.

The model employs a Monod-type interaction to describe species growth and nutrient dynamics. The organic pollutant P_0 is consumed by bacteria, fish, and aquatic plants according to the rates of $\frac{\beta_{20}P_oB}{\beta_{21}+\beta_{22}P_0}$. $\frac{k_1P_0F}{k_{12}+k_{11}P_o}$, and $\frac{\beta_{01}P_oA}{\beta_{12}+\beta_{11}P_o}$respectively. Oxygen is depleted during the decomposition of organic matter atthe rate of $\frac{\beta_{02}P_0B}{\beta_{21}+\beta_{22}P_0}$ while fish benefit from consuming P_0 at the rate $\frac{\lambda_4k_1P_0F}{k_{12}+k_{11}P_0}$.

We therefore formulate the model system of nonlinear differential equations presented as Eq. (1)

$$\begin{cases} \frac{dP_i(t)}{dt} = Q_1 - \alpha P_i F - \mu_1 P_i, \\ \frac{dP_0(t)}{dt} = Q_2 - \frac{\beta_{20}P_oB}{\beta_{21}+\beta_{22}P_o} - \frac{k_1P_oF}{k_{12}+k_{11}P_o} - \frac{\beta_{01}P_oA}{\beta_{12}+\beta_{11}P_o} - \mu_2 P_o, \\ \frac{dA(t)}{dt} = \Lambda_2 A + \frac{\lambda_3\beta_{01}P_oA}{\beta_{12}+\beta_{11}P_o} - \mu_3 A - \lambda_{30}A^2, \\ \frac{dB(t)}{dt} = A_3 B + \frac{\lambda_2\beta_{20}P_0B}{\beta_{21}+\beta_{22}P_0} - \lambda_{20}B^2, \\ \frac{dC(t)}{dt} = \Lambda - \frac{\beta_{02}P_oB}{\beta_{21}+\beta_{22}P_o} - \gamma_1 CF - \gamma_2 A - \gamma_3 B - \mu_4 C, \\ \frac{dF(t)}{dt} = \Lambda_1 F + \frac{\lambda_4 k_1 P_o F}{k_{12}+k_{11}P_o} + \gamma_1 CF - \theta P_I F - \mu_5 F - \lambda_{10}F^2. \end{cases} \tag{1}$$

2.2 Qualitative analysis

2.2.1 Positivity of the model solution

For the model system (1) to be ecologically and mathematically meaningful, we need to prove that all state variables are non-negative for all $t \geq 0$,

Lemma 2.1 *The solutions* $(P_i(t),\ P_o(t), B(t),\ A(t),\ F(t),\ C(t))$ *of the model system (1) with initial conditions* $P_i(0) > 0, P_o(0) > 0, B(0) > 0, A(0) > 0, C(0) > 0$ *and* $F(0) > 0$ *are positive for all* $t \geq 0$.

Proof. Considering the first equation of the model system (1), we have

$$\frac{dP_i}{dt} > -(\alpha F + \mu_1)P_i \tag{2}$$

Whose solution is given by

$$P_i(t) > P_i(0)e^{-(\alpha F+\mu_1)t}.$$

Likewise, the variables $P_o(t), A(t), B(t),\ C(t)$ and $F(t)$ can be computed following a similar procedure and establish that $P_o(t) > 0, B(t) > 0, A(t) > 0, F(t), C(t) > 0$ whenever $t \geq 0$. Therefore, the solution set $\left(P_i(t),\ P_o(t),\ A(t), B(t), C(t),\ F(t)\right) \in \mathbb{R}_+^6, \forall \geq 0$.

2.2.2 Boundness of the model

The model system (1) was developed taking into account the fields of biology, environment, epidemiology, and ecology, assuming that all the state variables and model parameters are well–posed for all $t \geq 0$. Initially, we demonstrate that the solutions of the model (1) are bounded as presented in Lemma 2.2.

Lemma 2.2 *The region of attraction for the model system (1) is contained in the following set:*

$$\Omega = \Big\{(P_i, P_o, A, B, C, F) \in \mathbb{R}_+^6 : 0 \leq P_i \leq \frac{Q_1}{\mu_1}, 0 \leq P_O \leq \frac{Q_2}{\mu_2}, 0 \leq A \leq L_A,$$

$$0 \leq B \leq L_B, 0 \leq C \leq \frac{\Lambda}{\mu_4}, 0 \leq F \leq L_F\Big\},$$

where

$$L_A = \frac{1}{\lambda_{30}}\left[\Lambda_2 - \mu_3 + \frac{\lambda_3\beta_{01}Q_2}{\mu_2\beta_{12} + \beta_{11}Q_2}\right], \frac{1}{\lambda_{20}}\left[\Lambda_3 - \mu_7 + \frac{\lambda_2\beta_{20}Q_2}{\mu_2\beta_{21} + \beta_{22}Q_2}\right]$$

and

$$L_F = \left[\frac{\lambda_4 k_1 Q_2}{\lambda_{10}(\mu_2 k_{12} + k_{11}Q_2)} + \frac{\Lambda_1\mu_1 + \gamma_1 L_C\mu_1 - \mu_5\mu_1}{\lambda_{10}\mu_1}\right].$$

Proof. Following Jha and Misra (2024), we will prove this lemma. From the first equation of model system (1), we establish that,

$$\frac{dP_i}{dt} \leq Q_1 - \mu_1 P_i, \tag{3}$$

whose solution is given by

$$\lim_{t\to\infty} \sup P_i \leq \frac{Q_1}{\mu_1},$$

Therefore, we have

$$0 \leq P_i \leq \frac{Q_1}{\mu_1}. \tag{4}$$

2.2.3 Equilibrium point analysis

To investigate the model's long-term dynamics, equilibrium points are determined by setting the growth rates of all state variables to zero, signifying steady-state solutions.

The system of equations (1) yields at least four feasible equilibrium points:

i. Equilibrium Point ξ_0

$\xi_0 = (0,0,0,0,0,0)$, representing a scenario devoid of pollutants, aquatic plants, bacteria, oxygen, and fish.

ii. Equilibrium Point ξ_1

$\xi_1 = \left(\frac{Q_1}{\mu_1}, \frac{Q_2}{\mu_2}, 0, 0, \frac{\Lambda}{\mu_4}, 0\right)$, where aquatic plants, bacteria, and fish are absent inthe system.

iii. Equilibrium Point ξ_2

$\xi_2 = (0, 0, A_2, B_2, C_2, F_2)$, corresponding to a pollutant-free water body. This exists under the conditions:

$$\begin{cases} \Lambda_2 - \mu_3 > 0, \\ \Lambda_3 - \mu_6 > 0, \\ \Lambda_1 - \mu_5 > 0, \\ 0 < \gamma_2 \left(\dfrac{\Lambda_2 - \mu_3}{\lambda_{30}}\right) + \gamma_3 \left(\dfrac{\Lambda_3 - \mu_6}{\lambda_{20}}\right) < \Lambda. \end{cases} \tag{5}$$

iv. Equilibrium Point ξ^*

$\xi^* = (P_i^*, P_o^*, A^*, B^*, C^*, F^*)$, indicating the coexistence of all species within the system.

Proof of the feasibility of these equilibria is in Appendix A.

2.2.4 Linear stability of equilibria

In this section, we conduct a local stability analysis of the equilibria for the model system (1) this analysis determines whether the system will settle into equilibrium when its state begins near, but not exactly at, an equilibrium point. An equilibrium is considered locally asymptotically stable if, for all initial conditions within a certain neighborhood around the equilibrium, the system converges to the equilibrium as time approaches infinity. The stability of an equilibrium is assessed by examining the sign of the real parts of the eigenvalues of the Jacobian matrix at the equilibrium point. Specifically, the equilibrium is stable if these eigenvalues are negative. The methods used to analyze the dynamical behavior of the model system (1) are detailed inAppendix B, providing insights into the stability and equilibrium properties of the system.

Concerning the local stability of all equilibria in system (1), we present the following theorem:

Theorem 1

1. *The equilibrium point ξ_0 is unstable provided the condition stated in equation 5 is satisfied.*
2. *The equilibrium point ξ_1 is unstable provided the condition stated in equation 5 is satisfied.*
3. *The equilibrium point ξ_3 is always unstable.*
4. *The equilibrium ξ^* is locally asymptotically stable if the following conditions hold:*

$$\begin{cases} (\alpha F^* + \mu_1)\left(\theta P_i^* + \mu_5 + 2\lambda_{10}F^* - \Lambda_1 - \dfrac{\lambda_4 k_1 P_o^*}{k_{12} + k_{11}P_o^*} + \gamma_1 C^*\right) > (\mu_1 P_i^* - m_5\theta F^*)^2, \\ m_2\left(\mu_3 + 2\lambda_{30}A^* - \Lambda_2 - \dfrac{\lambda_3\beta_1 P_o^*}{\beta_{12} + \beta_{11}P_o^*}\right)(\gamma_1 F^* + \gamma_3) > \dfrac{P_o^*(k_{11}P_o^* + k_{12})}{\lambda_4\gamma_1 k_{12}C^*}\gamma_2^2, \\ \left(\dfrac{\beta_{02}P_o^* B^*}{\beta_{21} + \beta_{22}P_o^*} + \mu_6 + 2\lambda_{20}B^* - \Lambda_3\right)(\mu_5 - \gamma_2) > \dfrac{P_o^*(k_{11}P_o^* + k_{12})}{\lambda_4\gamma_1 k_{12}C^*}\gamma_3^2. \end{cases} \tag{6}$$

The proof of this theorem is given in Appendix ***B.***

2.2.5 Nonlinear stability of interior equilibrium

In this section, we broaden our stability analysis from the small region near the equilibrium point to the entire region of attraction by employing Lyapunov's second method. The core concept of this approach for assessing the nonlinear stability of an equilibrium point is to identify an energy function that decreases over time along the system's trajectories. Given that the equilibriumξ^*, where all dynamic variables are active, is the most significant equilibrium among those in system (1), we will establish conditions for the global asymptotic stability ofξ^*.

Concerning the global stability of the equilibrium ξ^*in system (1), we present the following theorem:

Theorem 2 *The interior equilibrium* ξ^* *if it exists, it is non-linearly stable inside the region of attraction if the following conditions hold:*

$$m_5\theta^2 < \lambda_{10}(\mu_1 - \alpha L_F) \quad (7a)$$

$$\left(\frac{m_2\lambda_3\beta_1\beta_{12}}{(\beta_{12}+\beta_{11}P_o^*)(\beta_{12}+\beta_{11}L_{P_o})}\right)^2 < \frac{m_1\lambda_{30}\beta_{20}\beta_{21}L_B}{(\beta_{21}+\beta_{22}P_o^*)(\beta_{21}+\beta_{22}L_{P_o})}, \quad (7b)$$

$$\left(\frac{m_3\lambda_2\beta_{20}\beta_{21}}{(\beta_{21}+\beta_{22}P_o^*)(\beta_{21}+\beta_{22}L_{P_o})}\right)^2 \frac{m_1\lambda_{20}k_1k_{12}L_F}{(\beta_{21}+\beta_{22}P_o^*)(\beta_{21}+\beta_{22}L_{P_o})}, \quad (7c)$$

$$m_4\left(\frac{\beta_{20}\beta_{21}L_B}{(\beta_{21}+\beta_{22}P_o^*)(\beta_{21}+\beta_{22}L_{P_o})}\right)^2 \frac{m_1\beta_{01}\beta_{12}L_B}{(\beta_{12}+\beta_{11}P_o^*)(\beta_{12}+\beta_{11}L_{P_o})}, \quad (7d)$$

$$m_5\left(\frac{k_1k_{12}}{(k_{12}+k_{11}P_o^*)(k_{12}+k_{11}L_{P_o})}\right)^2 < \lambda_{10}\mu_2\,, \quad (7e)$$

$$m_4\gamma_2^2 < \lambda_{30}(\gamma_1 L_F - \gamma_4), \quad (7f)$$

$$m_5\gamma_1^2 < m_4\lambda_{10}(\gamma_1 L_F - \gamma_4). \quad (7g)$$

The proof of this theorem is given in Appendix C.

2.3 Quantitative analysis

2.3.1 Parameter estimation and model fitting

Following the examination of the asymptotic behaviors and long-term qualitative outcomes of the model system, parameter estimation becomes imperative for achieving precise quantitative predictions within a finite timeframe when constrained by empirical data. In this study, we utilized the least squares method for parameter estimation, suitable for general parameter calibration rather than hypothesis testing or confidence interval determination. The parameter values (refer to Table 1) were obtained by minimizing the sum of squared residuals $\left(min\sum_{i=1}^{n}(Y_g - Y_l)^2\right)$ between the model solutions (Y_l)derived from literature values and synthetic data (Y_g) generated by incorporating Gaussian noise into the model output (Y_l) Fanuel et al. (2023). The MATLAB built-in function fminsearch, which employs the Nelder-Mead simplex algorithm, was used to identify the local minimizers of the residual sum of squares. Initial parameter values were selected based on compliance with the conditions outlined in the qualitative analysis. The estimated parameters were applied to fit the data (Y_g), with the optimal fits depicted in Fig. 1. Furthermore, the autocorrelation of the residuals was analyzed, revealing an insignificant correlation at the 5% significance level (see Fig. 4). These results suggest that the estimated parameters yield the optimal fit for the data.

Table 1 Estimated parameter values.

Parameter	Initial value	Source	Estimated	Mean (μ) and std (σ)
Q_1	18.056	Tiwari et al. (2018)	18.002902	N 18.0832 3.84×10^{-2}
Q_2	18.056	Tiwari et al. (2018)	18.088006	N 18.0786 3.20×10^{-2}
Λ	16.913	Tiwari et al. (2018)	16.930407	N16.9228 1.38×10^{-2}
Λ_1	0.5	Assumed	0.503617	N 0.5003 3.78×10^{-4}
Λ_2	0.5	Assumed	0.493277	N 0.5038 5.41×10^{-3}
Λ_3	0.5	Assumed	0.515624	N 0.4966 4.74×10^{-3}
α	0.05	Assumed	0.049929	N 0.0500 2.50×10^{-5}
θ	0.02	Assumed	0.020310	N 0.0199 1.77×10^{-4}
λ_2	0.33	Tiwari et al. (2018)	0.336046	N 0.3288 1.76×10^{-3}
λ_3	0.2	Assumed	0.200531	N 0.2013 1.83×10^{-3}
λ_4	0.13	Assumed	0.131187	N 0.1307 9.69×10^{-4}
λ_{10}	0.446	Tiwari et al. (2018)	0.443490	N 0.4461 1.46×10^{-4}
λ_{20}	8.278	Tiwari et al. (2018)	8.373243	N 8.1913 1.23×10^{-1}
λ_{30}	0.5	Assumed	0.503893	N 0.5019 2.75×10^{-3}
β_{01}	0.029	Tiwari et al. (2019)	0.028717	N 0.0293 4.31×10^{-4}
β_{02}	0.112	Tiwari et al. (2018)	0.110319	N 0.1137 2.47×10^{-3}
β_{20}	4.38	Tiwari et al. (2017)	4.409343	N 4.4076 3.91×10^{-2}
β_{11}	0.051	Tiwari et al. (2019)	0.051012	N 0.0509 1.70×10^{-4}
β_{12}	1.0	Tiwari et al. (2019)	1.012754	N 0.9837 2.30×10^{-2}
β_{21}	7.81	Tiwari et al. (2017)	7.778490	N 7.8338 3.37×10^{-2}
β_{22}	1.48	Tiwari et al. (2017)	1.497801	N 1.4931 1.85×10^{-2}
k_1	1.0	Assumed	0.999306	N 0.9969 4.33×10^{-3}
k_{11}	1.0	Assumed	1.004568	N 1.0000 4.7×10^{-5}
k_{12}	1.0	Assumed	1.007983	N 0.9923 1.09×10^{-2}
μ_1	0.2	Assumed	0.199239	N 0.2000 2.5×10^{-5}
μ_2	1.804	Tiwari et al. (2018)	1.810026	N 1.8050 1.41×10^{-3}
μ_3	0.031	Assumed	0.031419	N 0.2997 4.22×10^{-4}
μ_4	0.3	Tiwari et al. (2018)	0.299548	N 0.0310 1.80×10^{-5}
μ_5	1.5	Tiwari et al. (2018)	1.498941	N 1.4986 1.92×10^{-3}
μ_6	0.28	Tiwari et al. (2018)	0.282797	N 0.2803 4.38×10^{-4}
γ_1	0.1	Tiwari et al. (2018)	0.100089	N 0.1000 3.50×10^{-5}
γ_2	0.5	Assumed	0.501070	N 0.5001 1.57×10^{-4}

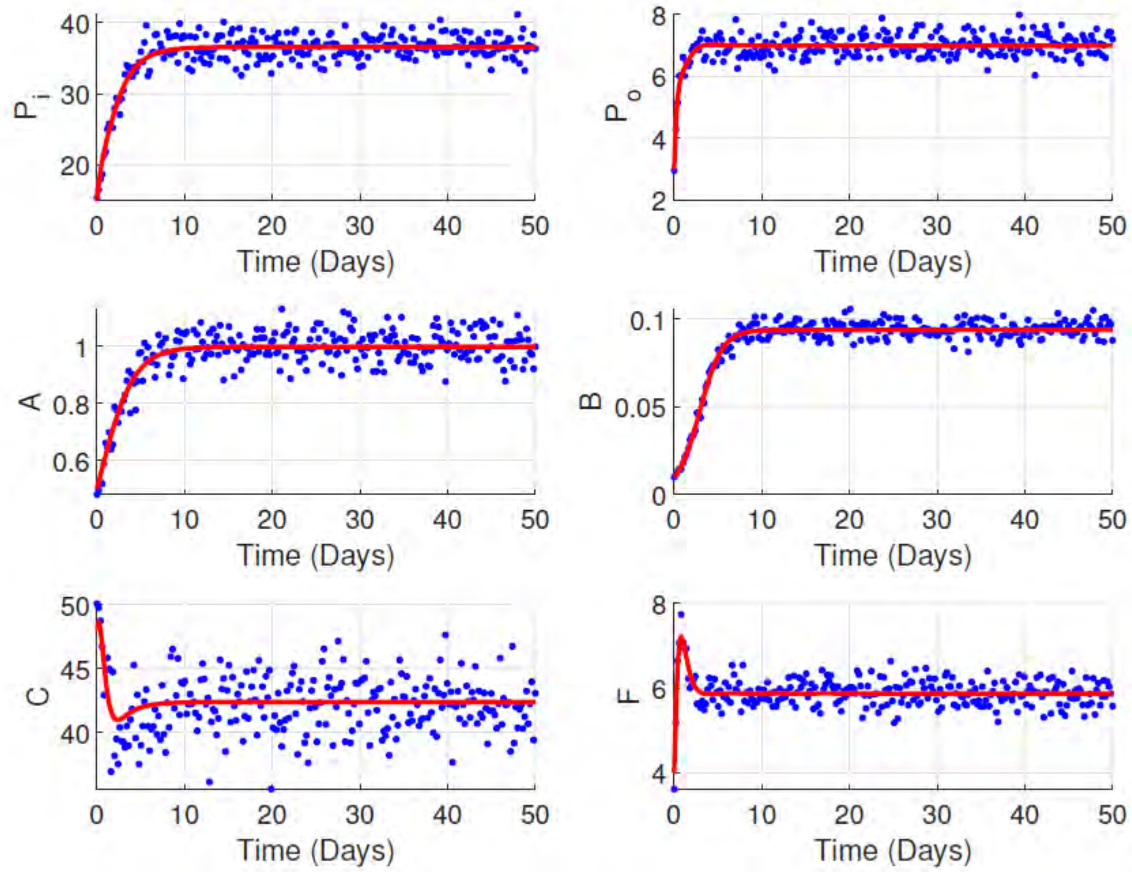

Fig. 1 Model fitting (lines) corresponding to estimated parameter values for Inorganic Pollutants(P_i), Organic Pollutants (P_o), Aquatic Plants (A), Bacteria (B), Oxygen Concentration (C) and Fish (F).

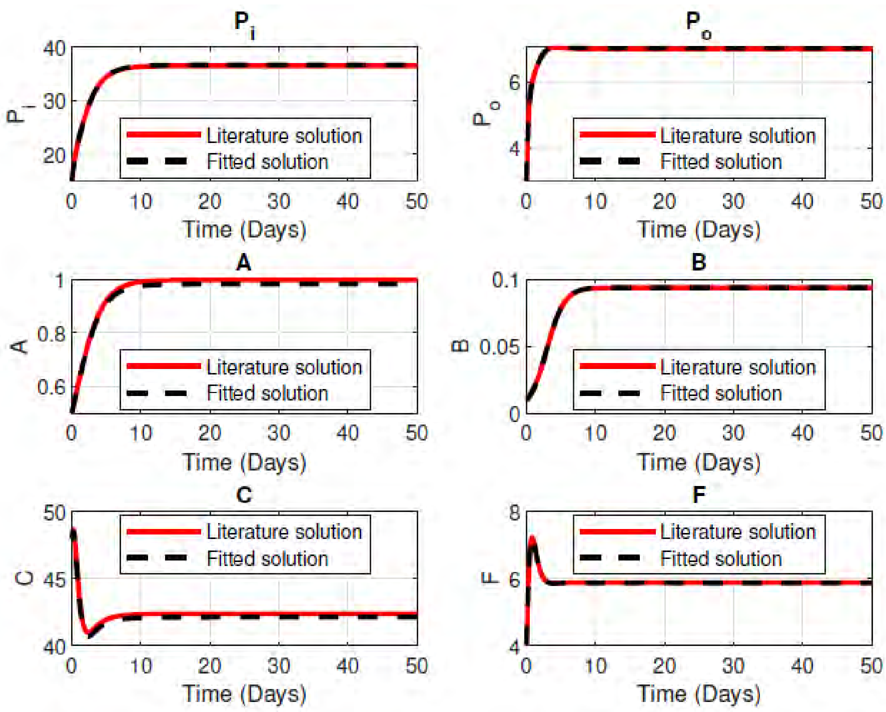

Fig. 2 Population dynamics using initial parameter values (in red sold line) and the best fit ofgenerated synthetic data (in black dashed) using Std = 0.05, in Inorganic Pollutants (Pi), OrganicPollutants (Po), Aquatic Plants (A), Bacteria (B), Oxygen Concentration (C) and Fish (F).

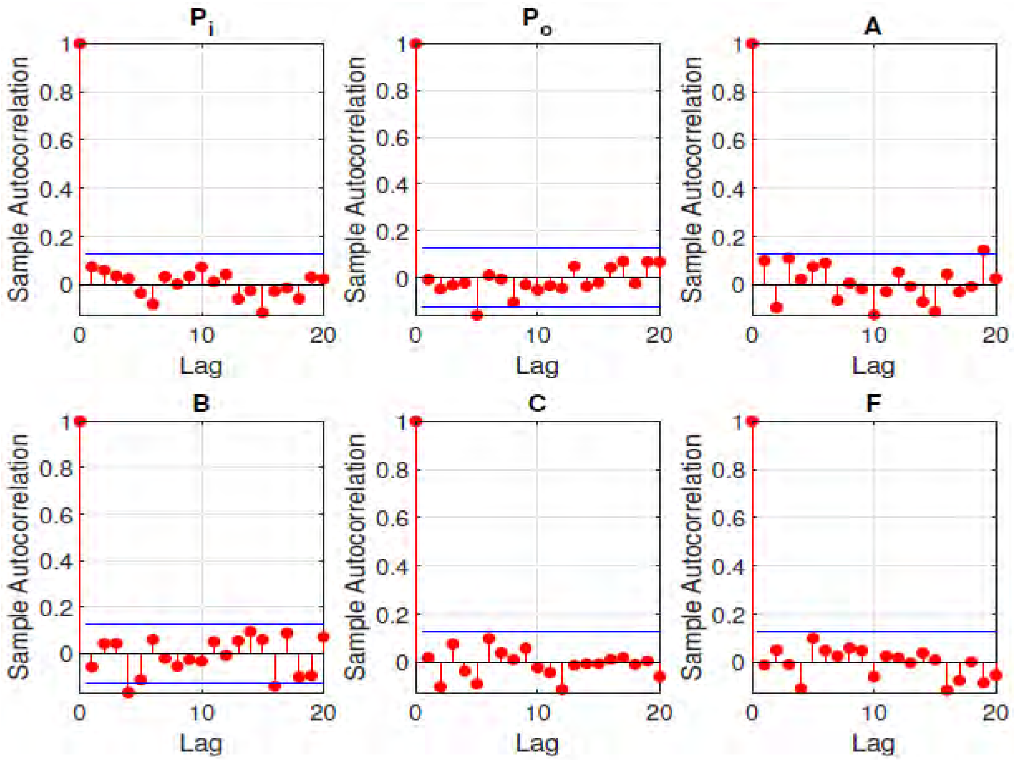

Fig. 3 The sample autocorrelation of the residuals in relation to Inorganic Pollutants (Pi), Organic Pollutants (Po), Aquatic Plants (A), Bacteria (B), Oxygen Concentration (C), and Fish Population (F).

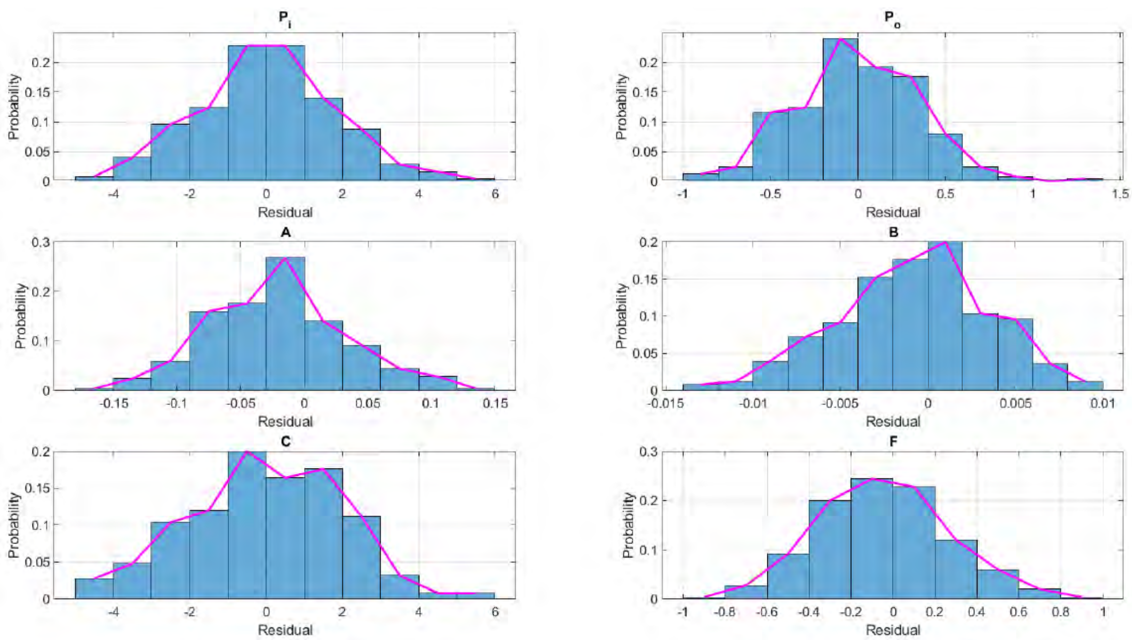

Fig. 4 Normal distribution of the model variables with standard deviation σ=0.05 and Confidence interval (C.I) =95%。

2.3.2 Sensitivity analysis

An exploratory analysis was carried out using time-varying sensitivity analysis, as no specific periods of interest were identified for the study. The analysis sought to identify meaningful time–dependent correlations spanning the entire period under investigation (Fanuel et al., 2023). The sensitivity of input parameters on the aquatic species, such as the aquatic plant population(A), bacteria population (B) and the fish population (F) was determined by plotting the PRCC values computed at various time intervals against time. The results of the analysis are presented in Figs. 5(a)–(c). From this figure, the shaded region represents PRCCs that are insignificantly different from zero $(-0.2 \leq PRCC \leq 0.2)$ (Marino et al., 2008).

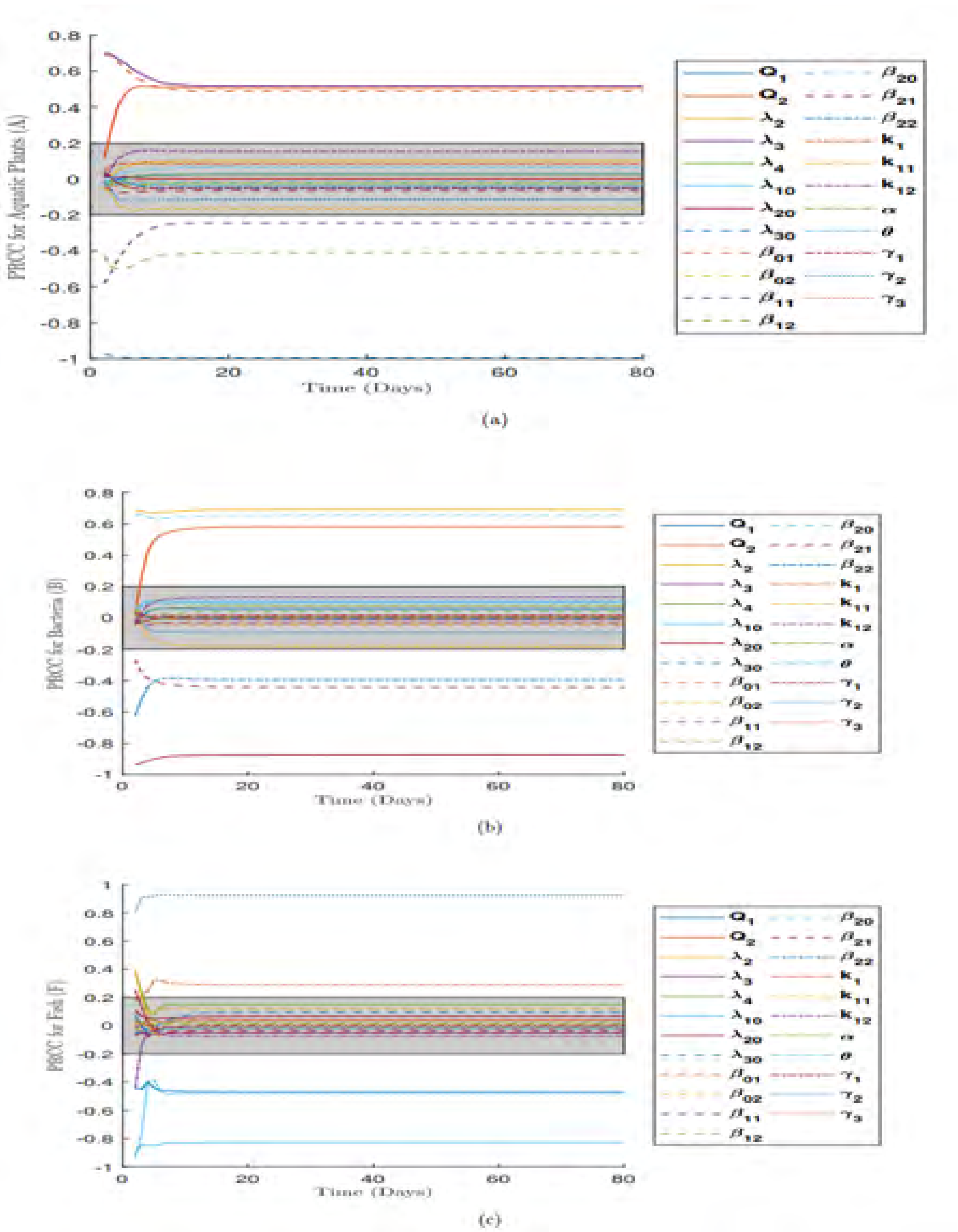

Fig. 5 A visual representation showing the evolution of parameter sensitivity throughout theprogression of the system dynamics. PRCC values over a time span of 80 days with respect to (a) Aquatic Plants, (b) Bacteria, and (c) Fish.

3 Results and Discussion

The model fitting and parameter estimation approach in this study provided a quantitative basis for understanding the aquatic ecosystems dynamics. Using the least squares method, the model's parameter values were adjusted to minimize the residuals between the model's predictions and the synthetic data, ensuring that the model fits the empirical data as closely as possible. Using the Nelder-Mead simplex algorithm via MATLAB's `fminsearch` function enabled efficient local minimization of residual sums, resulting in a good fit with insignificant residual autocorrelation.

The sensitivity analysis, conducted using Partial Rank Correlation Coefficients (PRCC) and Latin Hypercube Sampling (LHS), provided valuable insights into the time-dependent effects of various parameters on different components of the aquatic ecosystem. From Fig. 5(a), for aquatic plants (A), the sensitivity analysis revealed that the growth rate driven by organic pollutants (λ_3), the absorption rate of pollutants(β_{01}), and the discharge rate of organic pollutants (Q_2) they are highly influential parameters, positively impacting the aquatic plant population. These factors promote plant growth by enhancing nutrient availability and favorable conditions, leading to increased biomass. On the other hand, the death rate due to intraspecific competition (λ_{30}) and the half-saturation constant negatively affects the plant population. Intraspecific competition reduces the availability of resources among plants, limiting growth, while the half-saturation constant likely represents a threshold beyond which the effectiveness of nutrient uptake diminishes, further restraining population growth.

From Fig. 5(b) we can see the growth rate of bacteria (B) driven by organic pollutants (λ_2), the uptake rate of organic pollutants by bacteria (β_{20}), and the discharge rate of organic pollutants (β_{20}), are identified as positively sensitive parameters, meaning they are directly proportional to the increase in bacterial population. These parameters promote bacterial growth by providing essential resources and conditions that enhance bacterial proliferation. Conversely, negative sensitivity is observed in parameters such as the death rate of bacteria due to intraspecific competition (λ_{20}), and certain constants (β_{21}) and (β_{22}). These negatively sensitive parameters hinder bacterial population growth, with intraspecific competition limiting the available resources among bacteria, and the constants likely representing factors that negatively influence bacterial viability or resource acquisition. Considering Fig. 5(c) of the fish population, the analysis indicates that the fish population (F) is highly sensitive to both the uptake rate of organic pollutants (k_1) and the penetration rate of oxygen into water (λ_2), with both parameters showing a positive correlation. The increased absorption of organic pollutants by fish enhances their population, likely due to the role of certain organic pollutants as nutrients or energy sources that support fish growth and metabolic functions. Additionally, oxygen is essential for fish survival and growth, as it is fundamental to respiration and various metabolic processes (Abdel-Tawwab et al., 2019). Therefore, these two factors are critical in sustaining and promoting a healthy fish population. Conversely, the graph shows that the fish population (F) is negatively affected by the death rate due to the consumption of inorganic pollutants (θ), the discharge rate of inorganic pollutants (Q_1), and the death rate due to interspecific competition (λ_{10}). These parameters are negatively sensitive, meaning increases in any of them lead to a decrease in the fish population. This underscores the importance of controlling inorganic pollutant discharge and managing interspecific competition to sustain healthy fish populations in aquatic environments.

4 Conclusion

The model fitting and parameter estimation conducted in this study offer a robust quantitative foundation for understanding the complex dynamics of aquatic ecosystems. By applying the least squares method and the Nelder-Mead simplex algorithm, the model was finely tuned to align closely with empirical data, minimizing residuals and ensuring accuracy. Sensitivity analysis, using Partial Rank Correlation Coefficients (PRCC) and Latin Hypercube Sampling (LHS), highlighted the critical roles of various parameters in shaping the populations of aquatic plants, bacteria, and fish. Parameters such as the growth rates driven by organic pollutants, pollutant absorption rates, and oxygen penetration were identified as highly influential, positively affecting population growth by enhancing nutrient availability and metabolic processes. Conversely, factors like intraspecific and interspecific competition, along with the discharge and consumption of inorganic pollutants, were found to have negative impacts, underscoring the need for careful management of these parameters. The findings emphasize the importance of regulating pollutant levels and competition within aquatic environments to sustain and promote healthy ecosystem dynamics.

References

Abdel-Tawwab M, Monier MN, Hoseinifar SH, Faggio C. 2019. Fish response to hypoxia stress: growth, physiological, and immunological biomarkers. Fish physiology and biochemistry, 45: 997–1013. https:doi.org//10.1007/s10695-019-00614-9.

Ali H, Khan E, Ilahi I. 2019. Environmental chemistry and ecotoxicology of hazardous heavy metals: environmental persistence, toxicity, and bioaccumulation. Journal of Chemistry, 2019(1): 6730305. https:doi.org//10.1155/2019/6730305.

Bashir I., Lone F, Bhat RA, Mir SA, Dar ZA, Dar SA. 2020. Concerns and threats of contamination on aquatic ecosystems. In: Bioremediation and Biotechnology. Springer. https:doi.org//10.1007/978-3-030-35691-01

Cadotte MW, Carscadden K, Mirotchnick N. 2011. Beyond species: functional diversity and the maintenance of ecological processes and services. Journal of AppliedEcology, 48(5): 1079–1087. https:doi.org//10.1111/j.1365-2664.2011.02048.x

Chaturvedi A, Ramesh K, Vatsala G. 2017. A mathematical approach to study the effect of pollutants/toxicants in the aquatic environment. International Journal of Research-Granthaalayah, 5(4): 33–38. https:doi.org// 10.29121/granthaalayah.v5.i4RAST.2017.3299

Fanuel IM, Mirau S, Kajunguri D, Moyo F. 2023. Conservation of forest biomass andforest-dependent wildlife population: Uncertainty quantification of the model parameters. Heliyon. 9(6). https:doi.org//10.1016/j.heliyon.2023.e16948

Geist J, Hawkins SJ. 2016.Habitat recovery and restoration in aquatic ecosystems:current progress and future challenges. Aquatic Conservation: Marine andFreshwater Ecosystems, 26(5): 942–962. https:doi.org// 10.1002/aqc.2702

Glibert PM. 2017. Eutrophication, harmful algae, and biodiversity—challenging paradigms in a world of complex nutrient changes. Marine Pollution Bulletin, 124(2): 591–606. https:doi.org// 10.1016/j.marpolbul.2017.04.027

Hader DP, Banaszak AT, Villafane VE., Narvarte MA, Gonzalez RA, Helbling EW. 2020.Anthropogenic pollution of aquatic ecosystems: Emerging problems with global implications. Science of the Total Environment, 713: 136586. https:doi.org// 10.1016/j.scitotenv.2020.136586

Jan M, Hassan S, Ara A. 2022. Freshwater biodiversity: Indicators of eutrophication and pollution. Biodiversity of Freshwater Ecosystems, 263–284. https:doi.org// 10.1201/9781003277125-11

Jha A, Misra A. 2024. A robust role of carbon taxes towards alleviating carbon dioxide:a modeling study. Journal of Engineering Mathematics, 144(1): 20. https:doi.org//https://doi.org/10.1007/s10665-023-10327-x

Kalra P, Tangri S. 2020. Study of effects of toxicants and acidity on oxygen-dependent aquatic population: a mathematical model. International Journal of Mathematical Modeling and Numerical Optimisation, 10(3):

307–329.https:doi.org//https://doi.org/10.1504/IJMMNO.2020.108621

Kumar A, Agrawal A, Hasan A, Misra A. 2016. Modeling the effect of toxicant on the deformity in a subclass of a biological species. Modeling Earth Systems and Environment, 2(1): 1–14. https://doi.org//https://doi.org/10.1007/s40808-016-0086-x

Lucas L, Deleersnijder E. 2016. Timescale methods for simplifying, understanding,and modeling biophysical and water quality processes in coastal aquatic ecosystems: A review. Water, 12(10): 2717. https:doi.org//https://doi.org/10.3390/w12102717

Marino S, Hogue IB, Ray CJ, Kirschner DE. 2008. A methodology for performing global uncertainty and sensitivity analysis in systems biology. Journal of Theoretical Biology, 254(1): 178–196. https:doi.org//10.1016/j.jtbi.2008.04.011

Misra A. 2011. Modeling the depletion of dissolved oxygen due to algal bloom in a lake by takingholling type-iii interaction. Applied Mathematics and Computation, 217(21): 8367–8376. https:doi.org//10.1016/j.amc.2011.03.034.

Okeke ES, Okoye CO, Atakpa EO, Ita RE, Nyaruaba R. 2022. Microplastics in agroecosystems: impacts on ecosystem functions and food chain. Resources, Conservation and Recycling, 177: 105961. https:doi.org//10.1016/j.resconrec.2021.105961

Rainbow PS. 2007. Trace metal bioaccumulation: models, metabolic availability and toxicity. Environment international, 33(4): 576–582. https:doi.org//10.1016/j.envint.2006.05.007

Sarma D, Kumar D. 2024. Eutrophication in freshwater and its microbial implications. In: Handbook of Aquatic Microbiology. 194–209, CRC Press, USA. https:doi.org//10.1201/9781003408543-14

Shi H, Xu, F, Cheng J, Shi V. 2023. Exploring the evolution of the food chain under environmental pollution with mathematical modeling and numerical simulation.Sustainability, 15(13): 10232.2023. https:doi.org//10.3390/su151310232

Shukla J, Misra A, Chandra P. 2008. Mathematical modeling and analysis of the depletion of dissolved oxygen in eutrophied water bodies affected by organic pollutants. Nonlinear Analysis: Real World Applications, 9(5): 1851–1865. https:doi.org// 10.1016/j.nonrwa.2007.05.016

Su C, Jiang LQ, Zhang WJ. 2014. A review on heavy metal contamination in the soil worldwide: Situation, impact and remediation techniques. Environmental Skeptics and Critics, 3(2): 24-38

Tiwari PK, Bulai IM, Misra AK, Venturino E. 2017. Modeling the direct and indirect effects of pollutants on the survival of fish in water bodies. Journal of Biological Systems, 25(03): 521–543

Tiwari PK, Bulai IM, Bona F, Venturino E, Misra AK. 2018. Human population effects on the Ulsoor Lake fish survival. Journal of Biological Systems, 26(04): 603–632.https:doi.org//10.1142/S0218339018500274

Tiwari PK, Samanta S, Bona F, Venturino E, Misra AK. 2019. The time delays influence on the dynamical complexity of algal blooms in the presence of bacteria.Ecological complexity, 39: 100769. https:doi.org//10.1016/j.ecocom.2019.100769

Wurtsbaugh WA, Paerl HW, Dodds WK. 2019. Nutrients, eutrophication and harmful algal blooms along the freshwater to marine continuum. Wiley Interdisciplinary Reviews: Water, 6(5): 1373.https:doi.org//10.1002/wat2.1373

Yan ZQ, XJ Z. 2017. Model-independent parameter estimation. User Manual (2004). Water quality assessment and water quality management in the Pearl RiverDelta. Environmental Science and Pollution Research, 24(10): 8783–8794

Zhang WJ, Zhang XY. 2007. A forecast analysis on fertilizers consumption worldwide. Environmental Monitoring and Assessment, 133: 427-434

Appendices

Appendix A: Equilibrium Point ξ_2 and ξ^*

Existence of Pollutant-Free Equilibrium Point ξ_2

$$\begin{cases} (\Lambda_2-\mu_3-\lambda_{30}A_2)A_2=0, \\ (\Lambda_3-\mu_6-\lambda_{20}B_2)B_2=0 \\ \Lambda-\gamma_1 C_2F_2-\gamma_2 B_2-\mu_4 C_2=0, \\ (\Lambda_1-\gamma_1 C_2-\mu_5-\lambda_{10}F_2)F_2=0, \end{cases} \qquad (A1)$$

The first two equations yield $A_2=\frac{(\Lambda_2-\mu_3)}{\lambda_{30}}$ and $B_2=\frac{(\Lambda_3-\mu_6)}{\lambda_{20}}$ for $A_2,B_2\neq 0$.

From the fourth equation, with $F_2\neq 0$, we have $F_2\frac{(\Lambda_1-\mu_5)+\gamma_1 C_2}{\lambda_{10}}$, denoted as $F_1(C_2)=f_2$. Substituting A_2,B_2, and $F_1(c_2)$ into the third equation of (A1) gives another function of C_2:

$$f_2(C_2)=\Lambda-\gamma_1 C_2 f_1(C_2)-\gamma_2\left(\frac{\Lambda_2-\mu_3}{\lambda_{30}}\right)-\gamma_3\left(\frac{(\Lambda_3-\mu_6)}{\lambda_{20}}\right)-\mu_4 C_2=0. \qquad (A2)$$

The following results are established:

i. $f_2(0)=\Lambda-\gamma_2\left(\frac{\Lambda_2-\mu_3}{\lambda_{30}}\right)-\gamma_3\left(\frac{(\Lambda_3-\mu_6)}{\lambda_{20}}\right)>0$, given the condition:

$$0<\gamma_2\left(\frac{\Lambda_2-\mu_3}{\lambda_{30}}\right)+\gamma_3\left(\frac{(\Lambda_3-\mu_6)}{\lambda_{20}}\right)<\Lambda.$$

ii. $f_2\left(\frac{\Lambda}{\mu_4}\right)=-\gamma_1\left(\frac{\Lambda}{\mu_4}\right)f_1\left(\frac{\Lambda}{\mu_4}\right)-\gamma_2\left(\frac{\Lambda_2-\mu_3}{\lambda_{30}}\right)-\gamma_3\left(\frac{\Lambda_3-\mu_6}{\lambda_{20}}\right)<0.$

iii. $f_2'(C_2)=-\gamma_1 f_1(C_2)-\gamma_1 C_2 f_2'(C_2)-\mu_4<0.$

These results indicate that $f_2(C_2)$ possesses a unique non-negative solution C_2, with $0<C_2<\frac{\Lambda}{\mu_4}$. Hence, the equilibrium point $\xi_2=(0,0,A_2,B_2,C_2,F_2)$ exists under the conditions:

$$\begin{cases} \Lambda_2-\mu_3>0 \\ \Lambda_3-\mu_6>0 \\ \Lambda_1-\mu_5>0 \\ 0<\gamma_2\left(\frac{\Lambda_2-\mu_3}{\lambda_{30}}\right)+\gamma_3\left(\frac{(\Lambda_3-\mu_6)}{\lambda_{20}}\right)<\Lambda. \end{cases} \qquad (A3)$$

Existence of Interior Equilibrium Point $(\xi)^*$

The interior equilibrium $\xi^*$is determined by solving the following system of equations:

$$\begin{cases} 0 = Q_1 - \alpha P_i^* F^* - \mu_1 P_i^*, \\ 0 = Q_2 - \dfrac{\beta_{20} P_o^* B^*}{\beta_{21} + \beta_{22} P_0^*} - \dfrac{k_1 P_o^* F^*}{k_{12} + k_{11} P_o^*} - \dfrac{\beta_{01} P_o^* A^*}{\beta_{12} + \beta_{11} P_o^*} - \mu_2 P_o^*, \\ 0 = \Lambda_2 A^* + \dfrac{\lambda_3 \beta_{01} P_o^* A^*}{\beta_{12} + \beta_{11} P_o^*} - \mu_3 A^* - \lambda_{30} A^{*2}, \\ 0 = \Lambda_3 B^* + \dfrac{\lambda_2 \beta_{20} P_o^* B^*}{\beta_{21} + \beta_{22} P_o^*} - \mu_6 B^* - \lambda_{20} B^{*2} \\ 0 = \Lambda - \dfrac{\beta_{02} P_o^* B^*}{\beta_{21} + \beta_{22} P_o^*} - \gamma_1 C^* F^* - \gamma_2 A^* - \gamma_3 B^* - \mu_4 C^*, \\ 0 = \Lambda_1 F^* + \dfrac{\lambda_4 k_1 P_o^* F^*}{k_{12} + k_{11} P_o^*} + \gamma_1 C^* F^* - \theta P_i^* F^* - \mu_5 F^* - \lambda_{10} F^{*2}. \end{cases} \qquad (A4)$$

Given that all variables are positive, we can express P_i^* as a function of F^* using the first equation:

$$P_i^* = \frac{Q_1}{\alpha F^* - \mu_1} = f_3(F^*) \qquad (A5)$$

Similarly, we can define A^*, B^* and C^* as functions of P_i^* and F^*, respectively:

$$A^* = \left(\frac{\Lambda_2 - \mu_3}{\lambda_{30}} - \frac{\lambda_3 \beta_{01} P_o^*}{\lambda_{30}(\beta_{12} + \beta_{11} P_o^*)}\right) = f_2(P_o^*), \qquad (A6)$$

$$B^* = \left(\frac{\Lambda_3 - \mu_6}{\lambda_{20}} - \frac{\lambda_3 \beta_{02} P_o^*}{\lambda_{20}(\beta_{21} + \beta_{22} P_o^*)}\right) = f_5(P_o^*), \qquad (A7)$$

$$C^* = \frac{1}{\gamma_1 F^* - \mu_4}\left(\Lambda - \frac{\beta_{02} P_o^* f_5(P_o^*)}{(\beta_{21} + \beta_{22} P_o^*)} - \gamma_2 f_4(P_o^*)\right) = f_6(P_o^*, F^*). \qquad (A8)$$

Substituting these into the system, we derive the isoclines A9 and A10:

$$Q_2 - \frac{\beta_{20} P_o^* f_5(P_o^*)}{(\beta_{21} + \beta_{22} P_o^*)} - \frac{k_1 P_o^* F^*}{k_{12} + k_{11} P_o^*} - \frac{\beta_{01} P_o^* f_4(P_o^*)}{\beta_{12} + \beta_{11} P_o^*} - \mu_2 P_o^* = f_7(P_o^*, F^*). \qquad (A9)$$

$$(\Lambda_1 - \mu_5) + \frac{\lambda_4 k_1 P_o^*}{k_{12} + k_{11} P_o^*} + \gamma_1 f_6(P_o^*, F^*) - \theta f_3(F^*) - \lambda_{10} F^* = f_8(P_o^*, F^*). \qquad (A10)$$

From the isocline A9, the following deductions can be made

1. For $F^* = 0$, the function $f_7(P_o^*, 0)$ simplifies to $g_1(P_o^*)$:

$$Q_2 - \frac{\beta_{20} P_o^* f_5(P_o^*)}{(\beta_{21} + \beta_{22} P_o^*)} - \frac{\beta_{01} P_o^* f_4(P_o^*)}{\beta_{12} + \beta_{11} P_o^*} - \mu_2 P_o^* = g_1(P_o^*)$$

(a) For $P_o^* = 0, g_1(0) = Q_2 > 0$.

(b) For $P_o^* = \frac{Q_2}{\mu_2}$, we have:

$$g_1\left(\frac{Q_2}{\mu_2}\right) = -\left[\frac{\beta_{20}\left(\frac{Q_2}{\mu_2}\right) f_5\left(\frac{Q_2}{\mu_2}\right)}{\beta_{21} + \beta_{22}\left(\frac{Q_2}{\mu_2}\right)} + \frac{\beta_{01}\left(\frac{Q_2}{\mu_2}\right) f_4\left(\frac{Q_2}{\mu_2}\right)}{\beta_{12} + \beta_{11}\left(\frac{Q_2}{\mu_2}\right)}\right] < 0.$$

(c) It can be shown through appropriate calculations that g1′ (Po∗) < 0 if inequality (A11) is satisfied:

$$\frac{\beta_{20} P_o^* f_4(P_o^*) \beta_{22}}{(\beta_{21} + \beta_{22} P_o^*)^2} + \frac{\beta_{01} P_o^* f_3(P_o^*) \beta_{11}}{(\beta_{12} + \beta_{11} P_o^*)^2} <$$

$$\frac{\beta_{20} f_4(P_0) + \beta_{20} P_o^* f_o'(P_o^*)}{\beta_{21} + \beta_{22} P_o^*} + \frac{\beta_{01} f_3(P_o^*) + \beta_{01} P_o^* f_3'(P_o^*)}{\beta_{12} + \beta_{11} P_o^*} + \mu_2. \qquad (A11)$$

(d) The conditions (a)–(c) confirm that A9 has a unique positive solution for P_o^* in the interval $0 < P_o^* < \frac{Q_2}{\mu_2}$.

2. The derivative $\left(\frac{dP_o^*}{dF}\right)$ is negative, $\left(\frac{dP_o^*}{dF}\right) < 0$.

From the analysis of the isocline given in equation (A10), we can derive the following outcomes:

1. If $F^* = 0$, we denote the resulting function as $f_3(P_o^*, 0) = g_2(P_o^*)$. Hence,

$$(\Lambda_1 - \mu_5) + \frac{\lambda_4 k_1 P_o^*}{k_{12} + k_{11} P_o^*} + \gamma_1 f_6(P_o^*) - \frac{\theta Q_1}{\mu_1} = g_2(P_o^*). \qquad (A12)$$

(a) When $P_o^* = 0$, it follows that $g_2(0) < (0)$, provided the condition in (A13) is satisfied

$$(\Lambda_1 - \mu_5) + \gamma_i f_6(0) < \frac{\theta Q_1}{\mu_1}. \qquad (A13)$$

(b) For $P_o^* = \frac{Q_2}{\mu_2}$, we obtain $g_2\left(\frac{Q_2}{\mu_2}\right) > 0$, under the inequality in (A14):

$$(\Lambda_1 - \mu_5) + \frac{\lambda_4 k_1 \left(\frac{Q_2}{\mu_2}\right)}{k_{12} + k_{11}\left(\frac{Q_2}{\mu_2}\right)} + \gamma_1 f_6\left(\frac{Q_2}{\mu_2}\right) - \left(\frac{Q_1}{\mu_1}\right) > \frac{\theta Q_1}{\mu_1}. \qquad (A14)$$

(c) Differentiating $g_2(P_o^*)$ with respect to P_o^* gives:

$$g_2'(P_o^*) = \frac{\lambda_4 k_{11} k_{12}}{(k_{11} P_o^* + k_{12})^2} + \gamma_1 f_6'(P_o^*).$$

Considering the points in (a) through (c), we conclude that equation (A10) has a unique positive solution within the interval $0 < P_o^* < \frac{Q_2}{\mu_2}$.

2. The derivative $\left(\frac{dP_o^*}{dF^*}\right)_2 > 0$.

As a result, the equilibrium values of $P_o^*$and $F^*$are uniquely determined within the intervals $0 < P_o < L_{P_o}$ and $0 < F < L_F$, respectively, provided that $\left(\frac{dP_o}{dF}\right)_1 < 0$and $\left(\frac{dP_o}{dF}\right)_2 > 0$

Once P_o^* and $F^*$are known, the equilibrium values of $P_i^*, A^*, B^*$and C^* can be computed from equations (A5), (A6), (A7), and (A8), respectively.

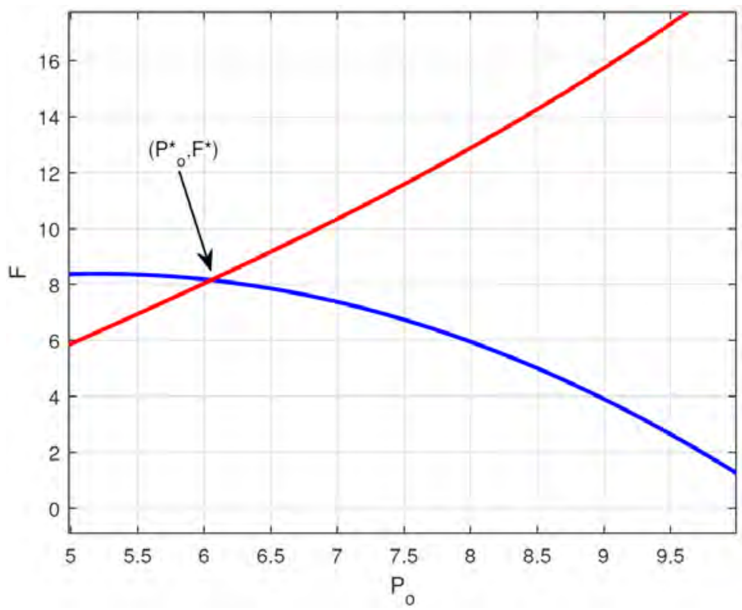

Fig. A1 The plot illustrates the intersection of the isoclines (A9) and (A10), signifying the presence of$(P_o{}^*F^*)$ within the interior of the first quadrant

Appendix B: Linear Stability of Equilibrium Points

The local stability of equilibrium points $\xi_0\xi_1$ and $\xi_2$of the model system (1) is analyzed by using the eigenvalue method, while the stability of an interior equilibrium point ξ^* is evaluated by using an appropriate Lyapunov candidate. The general Jacobian matrix (J) of the model system (1) is given by

$$J=\begin{bmatrix} J_{11} & 0 & 0 & 0 & 0 & J_{16} \\ 0 & J_{22} & J_{23} & J_{24} & 0 & J_{26} \\ 0 & J_{32} & J_{33} & 0 & 0 & 0 \\ 0 & J_{42} & 0 & J_{44} & 0 & 0 \\ 0 & J_{52} & 0 & J_{54} & J_{55} & J_{56} \\ J_{61} & J_{62} & 0 & 0 & J_{56} & J_{66} \end{bmatrix} \qquad (B15)$$

Where

$J_{11}=-\alpha F-\mu_1, J_{16}=-\alpha P_i,$

$J_{22}=-\left(\frac{\beta_{20}\beta_{21}B}{(\beta_{22}P_o+\beta_{21})^2}+\frac{k_1k_{12}F}{(k_{11}P_o+k_{12})^2}+\frac{\beta_{01}\beta_{12}A}{(\beta_{11}P_o+\beta_{12})^2}-\mu_2\right),$

$J_{23}=-\frac{\beta_{01}P_oB}{\beta_{12}+\beta_{11}P_o}, J_{24}=-\frac{\beta_{20}P_o}{\beta_{21}+\beta_{22}P_o}, J_{26}=-\frac{k_1P_o}{k_{12}+k_{11}P_o}, J_{32}=\frac{\lambda_3\beta_{01}A\beta_{12}}{(\beta_{11}P_o+\beta_{12})^2},$

$J_{33}=(\Lambda_2-\mu_3)+\frac{\lambda_3\beta_{01}P_o}{\beta_{12}+\beta_{11}P_o}-2\lambda_{30}A, J_{42}=\frac{\beta_{20}B\lambda_2\beta_{21}}{(\beta_{22}P_o+\beta_{21})^2},$

$J_{44}=(\Lambda_3-\mu_6)+\frac{\beta_{02}P_oB}{\beta_{21}+\beta_{22}P_o}-2\lambda_{20}B, J_{52}=\frac{\beta_{02}B\beta_{21}}{(\beta_{22}P_o+\beta_{21})^2}, J_{53}=-\gamma_2, J_{54}=-\gamma_3,$

$J_{55}=\gamma_2-\gamma_1F-\gamma_3-\mu_5, J_{56}=-\gamma_1C, J_{61}=\theta F, \quad J_{62}=\frac{\lambda_4k_1Fk_{12}}{(k_{11}P_o+k_{12})^2}, J_{65}=\gamma_1F,$

$J_{66}=(\Lambda_1-\mu_5)+\frac{\lambda_4k_1P_o}{k_{12}+k_{11}P_o}+\gamma_1C-\theta P_i-2\lambda_{10}F.$

Stability of Trivial Equilibrium ξ_0

Eigenvalues of the Jacobian matrix J evaluated at trivial equilibrium point, E0 are $-\mu_1, -\mu_1, (\Lambda_2 - \mu_3), (\Lambda_3 - \mu_6), \gamma_2 - \gamma_3 - \mu_5$ and $(\Lambda_1 - \mu_5)$. Conditions (A3) show that eigenvalues$(\Lambda_2 - \mu_3) > 0$ and $(\Lambda_3 - \mu_6) > 0$ respectively, suggesting instability of equilibrium point ξ_0.

Stability of Bacteria-Plants and Fish-Free Equilibrium Point ξ_1

Eigenvalues of the Jacobian matrix J evaluated at the Bacteria-Plants and fish free equilibrium point, ξ_1 are $-\mu_1, -\mu_1, (\Lambda_2 - \mu_3) + \frac{\lambda_3 \beta_{01} Q_2}{\beta_{12}\mu_2 + \beta_{11} Q_2}$, $(\Lambda_3 - \mu_6)$, $(\gamma_2 - \mu_5) - \gamma_3$, and

$(\Lambda_1 - \mu_5) + \frac{\lambda_4 k_1 Q_2}{k_{12}\mu_2 + k_{11} Q_2} + \gamma_1 C - \frac{\theta Q_1}{\mu_1}$. Conditions (A3) show that eigenvalues

$(\Lambda_2 - \mu_3) + \frac{\lambda_3 \beta_{01} Q_2}{\beta_{12}\mu_2 + \beta_{11} Q_2} > 0$ and $(\Lambda_3 - \mu_6) > 0$ which confirms that the equilibrium point ξ_1 is unstable.

Stability of Pollutants Free Equilibrium Pointξ_2

Eigenvalues of the Jacobian matrix J evaluated at the pollutant-free equilibrium pointE_2 are $-(\alpha_1 F_2 + \mu_1), \left(\frac{\beta_{20}\beta_2}{\beta_{21}} + \frac{k_1 F_2}{k_{12}} + \frac{\beta_{01} A_2}{\beta_{12}} + \mu_2\right), (\Lambda_2 - \mu_3) - 2\lambda_{30} A_2, (\Lambda_3 - \mu_6) - 2\lambda_{20} B_2, (\gamma_2 - \mu_5) - (\gamma_1 F_2 + \gamma_3), -\gamma_2 C_2, -\gamma_1 F_2,$ and $(\Lambda_1 - \mu_5) + \gamma_1 C_2 - 2\lambda_{10} F_2$,since$\gamma_1 F_2 > 0$,
the equilibrium $\xi_2$is unstable.

Stability of Coexistence Equilibrium Pointξ^*

Following Fanuel et al. (2023), we study the behavior of the system in the neighborhood of the equilibrium point when given a small perturbation.We begin by linearizing the system using the following transformations: $P_i = P_i^* + p_i, P_o = P_o^* + p_o, A = A^* + a, B = B^* + b, C = C^* + c$ and $F = F^* + f$,where$p_i, p_o, a, b, c,$ and $f$represent small perturbations around the equilibrium.
The linearlized system is given by

$$\frac{dp_i}{dt} = (-\alpha F^* + \mu_1) i - \mu_1 P_i^* f \ ,$$

$$\frac{dp_o}{dt} = \left(\frac{\beta_{20}\beta_{22} P_o^* B^*}{(\beta_{22} P_0^* + \beta_{21})^2} - \frac{\beta_{20} B^*}{\beta_{22} P_0^* + \beta_{21}} - \frac{k_1 F^*}{k_{11} P_o^* + k_{12}} + \frac{k_1 k_{11} P_o^* F^*}{(k_{11} P_o^* + k_{12})^2} - \frac{\beta_{01} A^*}{\beta_{11} P_o^* + \beta_{12}}\right) p_o - \left(\frac{\beta_{01} P_o^*}{\beta_{12} + \beta_{11} P_o^*}\right) a - \left(\frac{\beta_{20} P_o^*}{\beta_{21} + \beta_{22} P_0^*}\right) b - \left(\frac{k_1 P_o^*}{k_{12} + k_{11} P_o^*}\right) f \ ,$$

$$\frac{da}{dt} = \left(\frac{\lambda_3 \beta_1 \beta_{12} A^*}{(\beta_{11} P_o^* + \beta_{12})^2}\right) p_o + \left(\Lambda_2 + \frac{\lambda_3 \beta_1 P_o^*}{\beta_{12} + \beta_{11} P_o^*} - \mu_3 - 2\lambda_{30} A^*\right) a \ ,$$

$$\frac{db}{dt} = \left(\frac{\lambda_2 \beta_{20} \beta_{21} B^*}{(\beta_{22} P_o^* + \beta_{21})^2}\right) p_o + \left(\Lambda_3 - \frac{\beta_{02} P_o^* B^*}{\beta_{21} + \beta_{22} P_o^*} - \mu_6 - 2\lambda_{20} B^*\right) b,$$

$$\frac{dc}{dt} = -\left(\frac{\beta_{02} \beta_{21} B^*}{(\beta_{22} P_0^* + \beta_{21})^2}\right) p_o - \gamma_2 a - \gamma_3 b + (\gamma_2 - \gamma_1 F^* - \gamma_3 - \mu_5) c - \gamma_1 C^* f.$$

$$\frac{df}{dt} = \theta F^* p_i + \left(\frac{\lambda_4 k_1 k_{12} F^*}{(k_{11} P_o^* + k_{12})^2}\right) p_o + \gamma_1 F^*$$

$$+\left(\Lambda_1+\frac{\lambda_4 k_1 P_o^*}{k_{12}+k_{11}P_o^*}+\gamma_1 C^*-\theta P_i^*-\mu_5-2\lambda_{10}F^*\right)f. \qquad (B16)$$

Now, we consider the following positive definite function:

$$V=\frac{1}{2}\left(p_i^2+m_1p_o^2+\frac{m_2a^2}{A^*}+\frac{m_3b^2}{B^*}+m_4c^2+\frac{m_5f^2}{F^*}\right),m_i>0,i=1,\dots,5$$

and use a linearized model (B16) to get

$$\frac{dV}{dt}=-(\alpha F^*+\mu_1)P_i^2$$

$$-\left(\frac{m_1\beta_{01}A^*}{\beta_{11}P_o^*+\beta_{12}}+\frac{m_1\beta_{20}B^*}{\beta_{22}P_o^*+\beta_{21}}+\frac{m_1k_1F^*}{k_{11}P_o^*+k_{12}}-\frac{m_1\beta_{20}\beta_{22}B^*}{(\beta_{22}P_o^*+\beta_{21})^2}-\frac{m_1k_1k_{11}P_o^*F^*}{(k_{11}P_o^*+k_{12})^2}\right)P_o^2$$

$$-m_2\left(\mu_3+2\lambda_{30}A^*-\Lambda_2-\frac{\lambda_3\beta_1P_o^*}{\beta_{12}+\beta_{11}P_o^*}\right)a^2-m_3\left(\frac{\beta_{02}P_o^*B^*}{\beta_{21}+\beta_{22}P_o^*}+\mu_6+2\lambda_{20}B^*-\Lambda_3\right)b^2$$

$$-m_4(\gamma_1F^*+\gamma_3+\mu_5-\gamma_2)c^2-m_5\left(\theta P_i^*+\mu_5+2\lambda_{10}F^*-\Lambda_1-\frac{\lambda_4k_1P_o^*}{k_{12}+k_{11}P_o^*}-\gamma_1C^*\right)f^2$$

$$-(\mu_1P_i^*-m_5\theta F^*)p_if-\left(\frac{m_2\lambda_3\beta_1\beta_{12}A^*}{(\beta_{11}P_o^*+\beta_{12})^2}-\frac{m_1\beta_1P_o^*}{\beta_{12}+\beta_{11}P_o^*}\right)p_oa$$

$$-\left(\frac{m_1\beta_{20}P_o^*}{\beta_{21}+\beta_{22}P_0^*}-\frac{m_3\lambda_2\beta_{20}\beta_{21}B^*}{(\beta_{22}P_o^*+\beta_{21})^2}\right)p_ob-m_4\left(\frac{\beta_{02}\beta_{21}B^*}{(\beta_{22}P_o^*+\beta_{21})^2}\right)p_oc$$

$$-\left(\frac{m_1k_1P_o^*}{k_{12}+k_{11}P_o^*}-\frac{m_3k_1k_{12}F^*}{(k_{11}P_o^*+k_{12})^2}\right)p_of-m_4\gamma_2ac-m_4\gamma_3bc-(m_4\gamma_1C^*+m_5\gamma_1F^*)cf\,.$$

Select the values of $m_1=1, m_2=-\frac{m_1P_o^*(\beta_{11}P_o^*+\beta_{12})}{\lambda_3\beta_{12}A^*}, m_3=-\frac{m_1P_o^*(\beta_{22}P_o^*+\beta_{21})}{\lambda_2\beta_{21}B^*}$,

$m_4=-\frac{m_1P_o^*(k_{11}P_o^*+k_{12})}{\lambda_4\gamma_1k_{12}C^*}$, and $m_5=\frac{m_1P_o^*(k_{11}P_o^*+k_{12})}{\lambda_4\gamma_1k_{12}C^*}$ arbitrary, the time derivative of V becomes

$$\frac{dV}{dt}=-(\alpha F^*+\mu_1)P_i^2$$

$$+\left(\frac{\beta_{20}B^*}{\beta_{22}P_o^*+\beta_{21}}+\frac{k_1F^*}{k_{11}P_o^*+k_{12}}+\frac{\beta_{01}A^*}{\beta_{11}P_o^*+\beta_{12}}-\frac{\beta_{20}\beta_{21}P_o^*B^*}{(\beta_{22}P_o^*+\beta_{21})^2}-\frac{k_1k_{11}P_o^*F^*}{(k_{11}P_o^*+k_{12})^2}\right)p_o^2$$

$$+m_2\left(\mu_3-2\lambda_{30}A^*-\Lambda_2-\frac{\lambda_3\beta_1P_o^*}{\beta_{12}+\beta_{11}P_o^*}\right)a^2+m_3\left(\frac{\beta_{02}P_o^*B^*}{\beta_{21}+\beta_{22}P_o^*}+\mu_6+2\lambda_{20}B^*-\Lambda_3\right)b^2$$

$$+m_3\big((\gamma_1F^*+\gamma_3+\mu_5-\gamma_2)\big)c^2+m_5\left(\theta P_o^*+\mu_5+2\lambda_{10}F^*-\Lambda_1-\frac{\lambda_4k_1P_o^*}{k_{12}+k_{11}P_o^*}+\gamma_1C^*\right)f^2$$

$$+(\mu_1P_i^*-m_5\theta F^*)p_if-m_4\gamma_2ac-m_4\gamma_3bc$$

The criteria for $\frac{dV}{dt}$ to be negative definite, based on Sylvester's criterion, are as follows:

$$(\alpha F^*+\mu_1)\left(\theta P_o^*+\mu_5+2\lambda_{10}F^*-\Lambda_1-\frac{\lambda_4k_1P_o^*}{k_{12}+k_{11}P_o^*}+\gamma_1C^*\right)>(\mu_1P_i^*-m_5\theta F^*)^2\,,$$

$$m_2\left(\mu_3-2\lambda_{30}A^*-\Lambda_2-\frac{\lambda_3\beta_1P_o^*}{\beta_{12}+\beta_{11}P_o^*}\right)(\gamma_1F^*+\gamma_3)>\frac{P_o^*(k_{11}P_o^*+k_{12})}{\lambda_4\gamma_1k_{12}C^*}\gamma_2^2\,, \qquad (B17)$$

$$\left(\frac{\beta_{02}P_o^*B^*}{\beta_{21}+\beta_{22}P_o^*}+\mu_6+2\lambda_{20}B^*-\Lambda_3\right)(\mu_5-\gamma_2)>\frac{P_o^*(k_{11}P_o^*+k_{12})}{\lambda_4\gamma_1k_{12}C^*}\gamma_3^2\,. \qquad (B1)$$

A positive value for m2 can be selected from these inequalities, such that inequality B18 to be satisfied. Consequently, the time derivative of V is negative definite, confirming the linear stability of the coexistence equilibrium.

Appendix C: Non-Linear Stability of Coexistence Equilibrium Points

To demonstrate the global stability of the equilibrium ξ^*, we start with the following positive definite function, as proposed by Fanuel et al. (2023); Kalra and Tangri (2020):

$$W = \frac{1}{2}(P_i - P_i^*)^2 + \frac{m_1}{2}(P_i - P_i^*)^2 + m_2\left(A - A^* - A^* \ln\frac{A}{A^*}\right) +$$
$$m_3\left(B - B^* - B^* \ln\frac{B}{B^*}\right) + \frac{m_4}{2}(C_i - C)^2 + m_5\left(F - F^* - F^* \ln\frac{F}{F^*}\right)$$

where m1, m2, m3, m4, and m5 are positive constants. We establish that the function W is positive definite by proving $W\,(P_i, P_o, A, B, C, F) > 0$ within the interior of Ω and $W(P_i, P_o, A, B, C, F) = 0$ only at ξ^*.

By differentiating the above equation with respect to time t along the trajectories of the model system (1) and rearranging the terms, we obtain:

$$\frac{dW}{dt} = (P_i - P_i^*)\frac{dP_i}{dt} + m_1(P_o - P_o^*)\frac{dP_o}{dt} + m_2\left(\frac{A - A^*}{A}\right)\frac{dA}{dt} + m_3\left(\frac{B - B^*}{B}\right)\frac{dB}{dt} + m_4\left(\frac{C - C^*}{C}\right)\frac{dC}{dt} + m_5\left(\frac{F - F^*}{F}\right)\frac{dF}{dt}.$$

By differentiating this equation with respect to time t along the solutions of the model(1) and further rearranging terms, we proceed with the analysis.

$$\frac{dW}{dt} = -(\mu_1 - \alpha F)(P_i - P_i^*)^2 - \left[\frac{m_1\beta_{20}\beta_{21}B}{(\beta_{21} + \beta_{22}P_o^*) + (\beta_{21} + \beta_{22}P_o)} + \frac{m_1 k_1 k_{12} F}{(k_{12} + k_{11}P_o^*) + (k_{12} + k_{11}P_o)}\right.$$
$$\left. + \frac{m_1\beta_{01}\beta_{12}B}{(\beta_{12} + \beta_{11}P_o^*) + (\beta_{12} + \beta_{11}P_o)} + m_1\mu_2\right](P_o - P_o^*)^2 - m_2\lambda_{30}(A - A^*)^2 - m_3\lambda_{20}(B - B^*)^2$$
$$-m_4(\gamma_1 F - \gamma_4)(C - C^*)^2 - m_5\lambda_{10}(P_i - P_i^*)^2 - m_5\theta(P_i - P_i^*)(F - F^*)$$
$$-\left(\frac{m_2\lambda_3\beta_1\beta_{12}}{(\beta_{12} + \beta_{11}P_o)(\beta_{12} + \beta_{11}P_o^*)}\right)(P_o - P_o^*)(A - A^*)$$
$$-\left(\frac{m_3\lambda_2\beta_{20}\beta_{21}}{(\beta_{21} + \beta_{22}P_o)(\beta_{21} + \beta_{22}P_o^*)}\right)(P_o - P_o^*)(B - B^*)$$
$$-\left(\frac{m_4\beta_{20}\beta_{21}B}{(\beta_{21} + \beta_{22}P_o)(\beta_{21} + \beta_{22}P_o^*)}\right)(P_o - P_o^*)(C - C^*)$$
$$-\left(\frac{m_5 k_1 k_{12}}{(k_{12} + k_{11}P_o^*)(k_{12} + k_{11}P_o)}\right)(P_o - P_o^*)(F - F^*) - m_4\gamma_2(A - A^*)(C - C^*)$$
$$-m_5\gamma_1(C - C^*)(F - F^*).$$

$$\frac{dW}{dt} = -[a_{11}(P_i - P_i^*)^2 + a_{22}(F - F^*)^2 + a_{33}(A - A^*)^2 + a_{44}(B - B^*)^2 + a_{55}(C - C^*)^2$$
$$+a_{66}(F - F^*)^2 + a_{16}(P_i - P_i^*)(F - F^*) + a_{23}(P_o - P_o^*)(A - A^*) + a_{24}(P_o - P_o^*)(B - B^*)$$
$$+a_{25}(P_o - P_o^*)(C - C^*) + a_{26}(P_o - P_o^*)(F - F^*) + a_{35}(A - A^*)(C - C^*)$$
$$+a_{56}(C - C^*)(F - F^*)].$$

Where,

$a_{11} = (\mu_1 - \alpha F)$,

$a_{22} = \left[\frac{m_1\beta_{20}\beta_{21}B}{(\beta_{21} + \beta_{22}P_o^*)(\beta_{21} + \beta_{22}P_o)} + \frac{m_1 k_1 k_{12} F}{(k_{12} + k_{11}P_o^*)(k_{12} + k_{11}P_o)} + \frac{m_1\beta_{01}\beta_{12}B}{(\beta_{12} + \beta_{11}P_o^*)(\beta_{12} + \beta_{11}P_o)} + m_1\mu_2\right]$,

$a_{33} = \lambda_{30}$, $\quad a_{44} = \lambda_{20}$, $\quad a_{55} = m_4(\gamma_1 F - \gamma_4)$, $\quad a_{66} = m_5\lambda_{10}$

$$a_{16} = m_5\theta, a_{23} = \left(\frac{m_2\lambda_3\beta_1\beta_{12}}{(\beta_{12} + \beta_{11}P_o)(\beta_{12} + \beta_{11}P_o^*)}\right), a_{24} = \frac{m_3\lambda_2\beta_{20}\beta_{21}}{(\beta_{21} + \beta_{22}P_o)(\beta_{21} + \beta_{22}P_o^*)},$$

$$a_{25} = \left(\frac{m_4\beta_{20}\beta_{21}B}{(\beta_{21} + \beta_{22}P_o)(\beta_{21} + \beta_{22})}\right), a_{26} = \left(\frac{m_5k_1k_{12}}{(k_{12} + k_{11}P_o^*)(k_{12} + k_{11}P_o)}\right), a_{35} = m_4\gamma_{2,} a_{56} = m_5\gamma_1.$$

Sufficient conditions for $\frac{dW}{dt}$ to be negative definite, as determined by Sylvester's criterion, are given in 7a-7g.

Any positive values for m_1, m_2, m_3, m_4, and m_5 can be selected as long as these inequalities (7a-7g) are satisfied.